

PITA: Physics-Informed Trajectory Autoencoder

Johannes Fischer^{*,1}, Kevin Rösch^{*,1,2}, Martin Lauer¹, Christoph Stiller¹

Abstract—Validating robotic systems in safety-critical applications requires testing in many scenarios including rare edge cases that are unlikely to occur, requiring to complement real-world testing with testing in simulation. Generative models can be used to augment real-world datasets with generated data to produce edge case scenarios by sampling in a learned latent space. Autoencoders can learn said latent representation for a specific domain by learning to reconstruct the input data from a lower-dimensional intermediate representation. However, the resulting trajectories are not necessarily physically plausible, but instead typically contain noise that is not present in the input trajectory. To resolve this issue, we propose the novel Physics-Informed Trajectory Autoencoder (PITA) architecture, which incorporates a physical dynamics model into the loss function of the autoencoder. This results in smooth trajectories that not only reconstruct the input trajectory but also adhere to the physical model. We evaluate PITA on a real-world dataset of vehicle trajectories and compare its performance to a normal autoencoder and a state-of-the-art action-space autoencoder.

Index Terms—Autoencoder, Trajectory, Physics-informed, Loss, Generative Model, Data Augmentation

I. INTRODUCTION

The introduction of robotic systems into domains that were previously operated by humans enables a wide range of new applications, such as autonomous driving, robotic surgery, and automated manufacturing. However, these systems need to be able to operate safely and reliably in a wide range of scenarios, and their safety has to be proven before they can be deployed. This requires extensive testing and validation in a wide range of scenarios, in particular, including rare or dangerous edge cases that are difficult to encounter in real-world testing.

To address this challenge, generative models have been proposed to generate data for testing of robotic systems. These systems can be used to construct edge cases by augmenting a real-world dataset with generated data. Earlier generative models did not use an encoder to generate data, for instance, DALL-E generates images from text descriptions without using an encoder [1]. More recently, generative models have been proposed that use an encoder in their architecture. For example, the Stable Diffusion model uses an encoder extracted from an autoencoder trained in an unsupervised manner to generate high-resolution images from a low-dimensional latent space conditioned on context information [2]. Stable diffusion has been empirically shown to outperform previous generative models in terms of synthesized image quality.

Our goal is to develop an encoder that captures the physical properties of trajectories and hence is suitable for trajectory generation. To this end, we investigate trajectory autoencoders

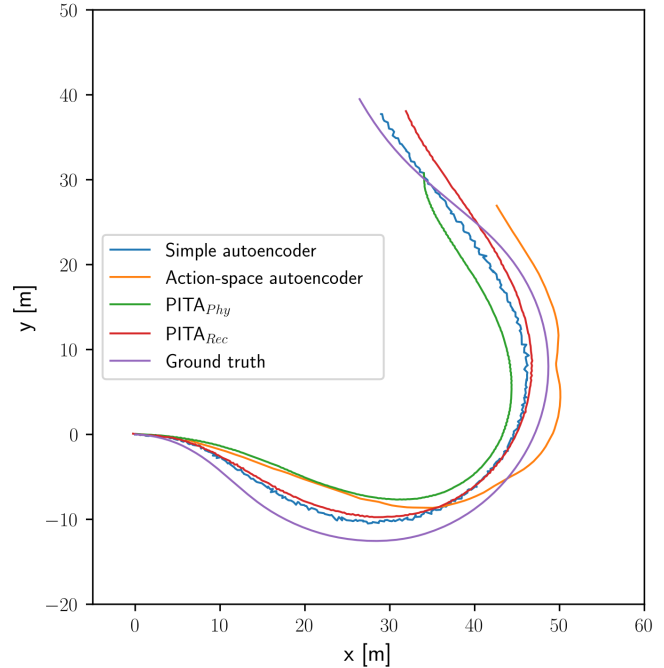


Figure 1: Comparison of different trajectory reconstruction methods resulting in more or less smooth trajectories.

which encode trajectories in a lower-dimensional latent space. The autoencoder is trained to reconstruct the input trajectory from the latent space, and can be used to generate new trajectories by sampling from the latent space. While being out of the scope of this work, the trained encoder can be used to construct a more involved generative trajectory model based on the learned latent space representation.

The problem with traditional trajectory generation is that the resulting trajectories are not necessarily physically plausible. The loss function is usually defined as the mean squared error between the input and the output trajectories. This results in a rather good reconstruction of the input trajectory, but the output trajectory still contains jitter and noise that is not present in the input trajectory and make it non-smooth, as the example in fig. 1 illustrates. This is particularly problematic if the predicted points have a high temporal resolution, as is required for generating edge cases: The motion between two adjacent points will not be physically plausible due to the noise-induced jitter. The training process does not capture the underlying physics of the system, but rather learns to reproduce the points almost independently of each other.

To address this issue, we propose to incorporate a physical model into the loss function of the autoencoder. The physical

^{*}equal contribution, names ordered alphabetically

¹Karlsruhe Institute for Technology {firstname.lastname}@kit.edu

²Research Center for Information Technology

model captures the system’s motion dynamics to ensure that the predicted trajectories are smooth and physically plausible. This gives rise to the physical loss, measuring how much the predicted trajectory violates the physical model. The loss function is defined as a combination of the reconstruction loss and the physical loss. Besides the loss function, the whole autoencoder architecture remains unchanged. This implies that our proposed loss can be added to any existing network architecture to improve the physical plausibility of the generated trajectories. The contributions of our work are threefold:

- We propose the Physics-Informed Trajectory Autoencoder (PITA), which uses a novel loss function that incorporates a physical model of the robotic system.
- We evaluate PITA on a real-world dataset of vehicle trajectories and propose metrics for evaluating the smoothness of a trajectory.
- We compare our approach to a traditional autoencoder and a state-of-the-art action-space based autoencoder [3].

II. RELATED WORK

Action-Space Prediction

Trajectory prediction is a well-established research area in robotics. Action-space prediction is an approach that allows to consider a dynamics model of the system [3], [4]. Those approaches use machine learning models to predict the future control inputs of the system. These control inputs are then used to integrate the dynamics model to predict the future trajectory. The model is trained to minimize the mean squared error between the resulting integrated trajectory and the ground truth trajectory. As a result, the prediction is implicitly guaranteed to satisfy the dynamics model.

Physics-Informed Neural Networks

An alternative to incorporate physical models into the learning process is given by Physics-Informed Neural Networks (PINNs) [5]. These models are trained to output the quantities of interest directly, while using a physical relationship as a regularization. This way, the neural network learn to output predictions that satisfy the physical model.

Physics-informed machine learning can benefit training with limited data, since the physical model provides additional information in between data points. Similarly, it also aids generalization to unseen scenarios, since the physical relation can be extrapolated to new situations.

Previous work has used physics-informed machine learning to incorporate driver models into imitation learning [6], [7] and reinforcement learning [8] for automated driving. The policies were trained to perform well, but also to be similar to the driver model guidance. This resulted in better performance on unseen data, thus alleviating the problem of covariate shift. In contrast to our work, the physical models these works used are not actual models derived from vehicle kinematics, but rather proxy models for car-following behavior.

Another work uses the kinematic bicycle model to [9] learn vehicle dynamics for off-road terrain. A neural network is trained to predict the future trajectory using a regression loss

for predicted points and a physics loss to make the predictions adhere to the kinematic bicycle model. They use the distance between predictions from the neural network and predictions from the bicycle model as physical loss. This is in contrast to our work, where the physical loss is composed of the error in the differential equation that described the kinematic bicycle model, and hence also penalizes non-smooth predictions.

III. METHOD

A. Physical Model

To achieve smooth trajectory predictions, we use the three degree-of-freedom kinematic bicycle model (KBM) as a physical regularization. Since we do not consider datasets with high-speed maneuvers, the KBM is sufficient to capture the vehicle dynamics. Usually, the KBM is formulated with the state \mathbf{x} consisting of the vehicle’s Cartesian position (x, y) , the heading angle θ and the velocity v . The control inputs \mathbf{u} are the steering angle δ and the acceleration a . The KBM relates the state and control inputs to the state derivatives using the wheelbase.

Since we train our approach on a real-world recorded dataset of vehicle trajectories from different vehicles, we do not have access to each vehicle’s wheelbase and steering angle. For this reason, we use the curvature κ as an input variable instead of the steering angle δ . This allows to formulate motion model independent of the vehicle’s wheelbase as

$$\frac{d\mathbf{x}}{dt} = \frac{d}{dt} \begin{bmatrix} x \\ y \\ \theta \\ v \end{bmatrix} = \begin{bmatrix} v \cos(\theta) \\ v \sin(\theta) \\ v\kappa \\ a \end{bmatrix} = f(\mathbf{x}, \mathbf{u}) \quad (1)$$

using the state $\mathbf{x} = (x, y, \theta, v)$ and control inputs $\mathbf{u} = (\kappa, a)$.

B. Loss definition

Reconstruction loss For one trajectory of length T , the reconstruction loss is given by the squared distance of corresponding predicted and ground truth trajectory points.

$$L_{\text{Rec}} = \sum_{t=1}^T \left\| \begin{pmatrix} \hat{x}_t \\ \hat{y}_t \end{pmatrix} - \begin{pmatrix} x_t \\ y_t \end{pmatrix} \right\|^2 \quad (2)$$

Physical loss

$$L_{\text{Phy}} = w_1 \left\| \frac{d\hat{x}}{dt} - \hat{v} \cos \hat{\theta} \right\|^2 + w_2 \left\| \frac{d\hat{y}}{dt} - \hat{v} \sin \hat{\theta} \right\|^2 \quad (3)$$

$$+ w_3 \left\| \frac{d\hat{\theta}}{dt} - \hat{v} \hat{\kappa} \right\|^2 + w_4 \left\| \frac{d\hat{v}}{dt} - \hat{a} \right\|^2 \quad (4)$$

$$+ w_5 \|\hat{\kappa}\|^2 + w_6 \|\hat{a}\|^2 \quad (5)$$

The terms in eqs. (3) and (4) are the errors in the differential equation, while the terms in eq. (5) are regularization terms to prevent the model from using excessive accelerations and curvatures.

Loss weighting: Since the terms of the physical loss have different units, we need to scale them to have similar magnitudes. To this end, we empirically tune the weights

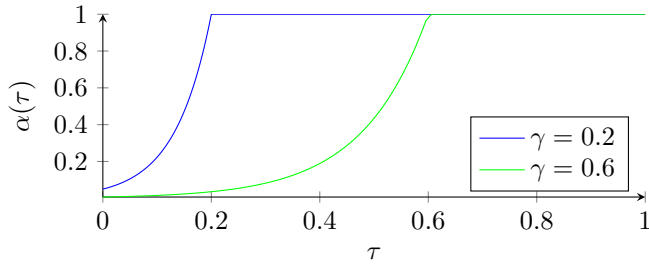


Figure 2: Physical loss weight scheduling scheme for different parameter values of γ .

w_1, \dots, w_6 to balance the contributions of the different terms in the physical loss.

Additionally, we also need to balance the contributions of the reconstruction loss and the physical loss. To this end, we introduce hyperparameters λ_1 and λ_2 for the two loss term.

In preliminary experiments, we observed that the model is prone to collapsing to zero predictions if λ_2 is too large, since a zero prediction results in zero physical loss. To resolve this, we have implemented a scheduling scheme for the physical loss, where we start with a small value and increase it exponentially over time during training, until it reaches its maximum value. The employed scheduling scheme is given by

$$\alpha(\tau) = \min\left(1, e^{m\left(\frac{\tau}{\tau_{\max}} - 1\right)}\right) \quad (6)$$

where τ is the current training step, τ_{\max} is the maximum number of training steps, m is a scaling factor which influences the shape of the increase and γ is the fraction of training steps after which the parameter reaches its maximum value.

Figure 2 illustrates the weight scheduling scheme α for different parameters values with $m = 5$ and $\gamma \in \{0.2, 0.6\}$. The final trajectory loss in training step τ is then given by

$$L(\tau) = \lambda_1 L_{\text{Rec}} + \alpha(\tau) \lambda_2 L_{\text{Phy}}. \quad (7)$$

IV. EVALUATION

A. Experimental Setup

Dataset: To evaluate our method, we use a real-world dataset of vehicle trajectories. Different trajectory datasets of preprocessed drone recordings are available to the research community [10]–[12]. To be able to augment data with generated trajectories at a high frame rate, we use a dataset that contains trajectories with high temporal resolution. Since we are interested in how well our model can capture the vehicle dynamics model, highway trajectories that are mostly straight are of less interest. For this reason, we chose the roundD dataset for our evaluation, which contains vehicles trajectories in roundabouts [11]. More precisely, it is composed of 13509 vehicle trajectories at three different locations with a total recorded time of over six hours, sampled with 25 Hz, i.e. at time steps of $\Delta t = 0.04$ s.

Preprocessing: A data point for our training is made up of a trajectory of one vehicle. Generally, it would be interesting to reconstruct the trajectories for all vehicles in the traffic scene

given the map context. However, since our main goal is to investigate the benefits of incorporating a physical model into the learning process, we chose to use single vehicle trajectories as input for the autoencoder. The trajectories are represented by the Cartesian positions of the vehicle at each time step. We translate all trajectories to start at the origin and rotate them to have the same initial orientation. As our autoencoder model has a fixed input dimension, we cut the trajectories to a fixed length of $T = 350$ time steps, which corresponds to a duration of 14 seconds. Since each point consists of x- and y-position, our model has an input dimension of $2 \cdot T = 700$.

Autoencoder architectures: We compare three different autoencoder architectures, which share the same architecture, but differ only in their output representations and loss functions. The autoencoder model follows the traditional network layout, we chose a depth of 12 layers for the encoder and decoder. The latent space has a fixed dimension of 320. This results in a total of round about 8 million parameters.

- 1) *Simple autoencoder:* The first baseline is a regular autoencoder where the output has the same dimension as the input and represents the reconstructed trajectory positions. It is trained to minimize the mean squared error between the input trajectory positions and the predicted trajectory positions.
- 2) *Action-space autoencoder:* The second baseline is an action-space autoencoder, based on the architecture proposed by Janjos et al. [3]. For the action-space autoencoder, the model output has a dimension of $2 \cdot T + 4$. The first four entries represent the predicted initial state of the vehicle $\hat{\mathbf{x}}_0 = (\hat{x}_0, \hat{y}_0, \hat{\theta}_0, \hat{v}_0)$ while the remaining elements are the predicted control inputs $\hat{\mathbf{u}}_t = (\hat{k}_t, \hat{a}_t)$ for the dynamics model at each time step t . Using these predicted control inputs, we integrate the vehicle dynamics model to obtain the predicted state trajectory using a fourth order Runge-Kutta method starting from the predicted initial state. The loss function is defined as the mean squared error between the input trajectory and the positions of the predicted state trajectory.
- 3) *Physics-informed autoencoder:* Our physics-informed trajectory autoencoder (PITA) has an output dimension of $6 \cdot T$, representing the predicted state and control input trajectory $(\mathbf{x}_t, \mathbf{u}_t)_{t=1}^T$. Based on the predicted states and control inputs, we compute the total loss as the weighted sum of the reconstruction loss between input trajectory and predicted positions and the physical loss as described in section III-B. To compute the physical loss, we approximate the state derivatives using central finite differences on the model outputs.

Training: All networks are trained with trajectories provided by the dataset described in section IV-A. The dataset is split into a training and a validation set, where we use the same split for all training runs to ensure comparability. In each training epoch, we train on randomly samples mini-batches using the mean squared error over a training batch as the loss function.

Model	Hyperparameters		
	$\lambda_1 [10^{-4}]$	$\lambda_2 [10^{-2}]$	γ
PITA _{Rec} (ours)	1.976	1.028	0.595
PITA _{Phy} (ours)	1.030	3.012	0.032

Table I: Comparison of hyperparameters for the physics-informed models.

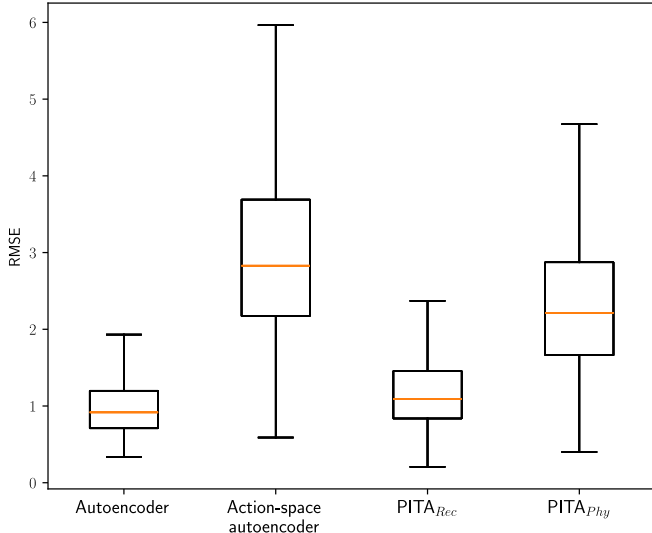


Figure 3: Reconstruction root mean squared error on the validation dataset.

We have run a hyperparameter search to find the best hyperparameters for the simple autoencoder and the action-space autoencoder based on the loss L_{Rec} on the validation set. To optimize the hyperparameters for PITA, we have run a hyperparameter search using the loss L as defined in eq. (7) on the validation set. This hyperparameter search produced different models on the Pareto frontier where the prediction performance qualitatively tended to go either in the direction of better reconstruction or better alignment with the physical model. We refer to these models as PITA_{Rec} and PITA_{Phy}, respectively. For the final training we fixed $m = 5$ used the hyperparameters that produced the best results in the hyperparameter search, which are provided in table I.

B. Comparison to Baseline Models

To evaluate our approach we consider two orthogonal aspects:

- 1) How well does the model reconstruct the input trajectory?
- 2) How physically plausible is the reconstructed trajectory?

Reconstruction error:

First and foremost, we compare how well our model is able to reconstruct the input trajectory in comparison to the baseline models. To this end, we measure the reconstruction in terms of the root mean squared error (RMSE) between predicted and ground truth positions on the validation dataset.

As fig. 3 illustrates, the simple autoencoder has the lowest reconstruction error, closely followed by PITA_{Rec}, which placed a higher emphasis on the reconstruction loss term. Our PITA_{Phy} model has a higher reconstruction error because it focuses more on the physical loss term. We can also observe, that the action-space autoencoder has the highest reconstruction error.

Physical plausibility:

To measure the adherence to the physical dynamics model, we experimented with different metrics. For the first one, we compute the KBM state and input trajectory solely from the positions predicted by the models using central finite differences. That is, we approximately compute the input trajectory that is necessary to follow the predicted trajectory with a KBM. The resulting values for absolute acceleration and curvature are an indicator for how physically plausible the predicted trajectory is. Excessive use of control inputs compared to the ground truth indicates that the predicted trajectory is not physically plausible.

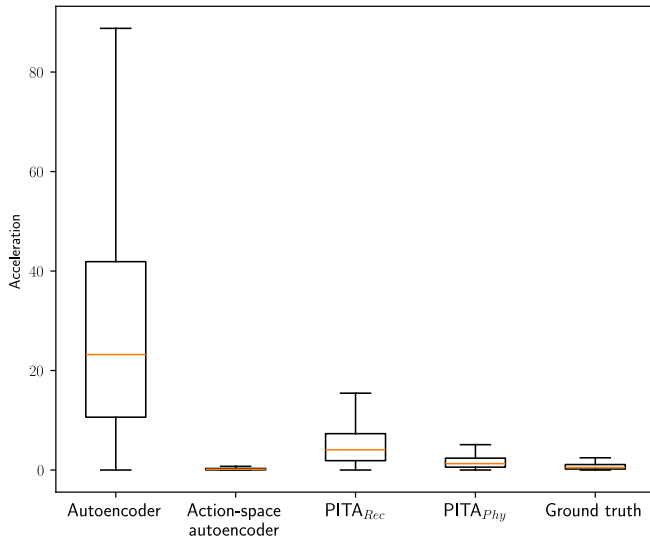
Figure 4 shows that the simple autoencoder model requires unrealistically high model inputs to follow the predicted trajectory, indicating the poor physical properties of its predictions. On the contrary, the action-space autoencoder does not make use of excessive control inputs. Both our PITA models are in between those two extremes, where the model that put more weight on the physical loss term requires less control inputs. While our models require more control inputs compared to the action-space autoencoder, they need drastically less control inputs than the simple autoencoder. We also show the computed model inputs for the ground truth trajectory as a reference.

As a second metric, we evaluate the smoothness of the predicted trajectory. Predicted trajectories that are physically implausible because of noise or jitter are expected to be less smooth than trajectories that do adhere to a physical motion model. To measure the smoothness, we first compute a smoothed reference path for every predicted trajectory using an Unscented Kalman Filter (UKF) [13] based on the KBM dynamics. We then compute the average distance of the predicted positions to the smoothed reference path as a measure for how smooth the predicted trajectory is.

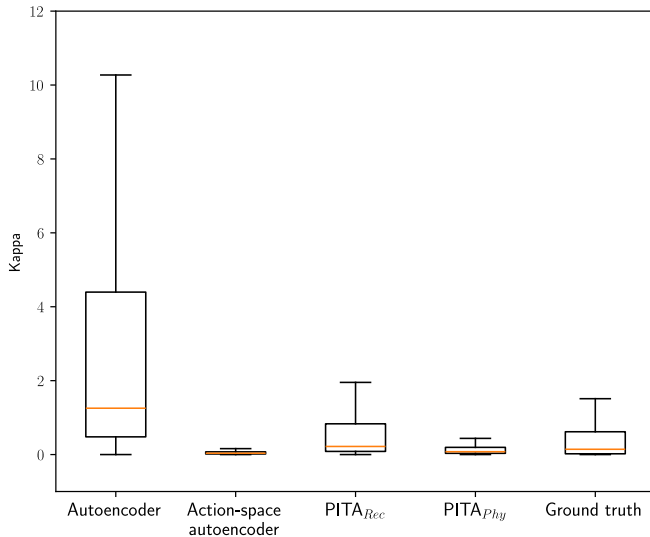
The results are displayed as a boxplot in fig. 5. We observe that the autoencoder model has the highest distance to the smoothed reference path, indicating that the predicted trajectory is less smooth. As expected, the action-space autoencoder has a very low distance to the smoothed reference path, since it satisfies the KBM by design. The two PITA models are again in between the two baseline models, with the PITA_{Phy} model having a lower distance to the smoothed reference path. This is again expected, due to the higher weight placed on the physical loss term. The values computed for the ground truth trajectory are between the action-space autoencoder and PITA_{Phy}.

V. CONCLUSION

One problem with high fidelity trajectory autoencoders is that due to the inherent noise they produce physically



(a) Absolute acceleration



(b) Absolute curvature

Figure 4: Boxplot of the model inputs necessary to follow the trajectories predicted by the different models with a KBM.

implausible trajectories. To resolve this issue, we propose a novel approach to encode and reconstruct vehicle trajectories using a combination of autoencoders and physics-informed machine learning. Our approach augments the reconstruction loss with a physics-based loss that enforces the reconstructed trajectories to adhere to a model of the system dynamics. We evaluate our approach on a real-world dataset and compare it to a standard autoencoder and an action-space autoencoder. The standard autoencoder produces the lowest reconstruction error but also the noisiest trajectories. On the contrary, the action-space autoencoder baseline achieves a smooth trajectory but at the cost of a higher reconstruction error. Our evaluation proves empirically that our approach can balance the two objectives and produce smooth and physically plausible trajectories.

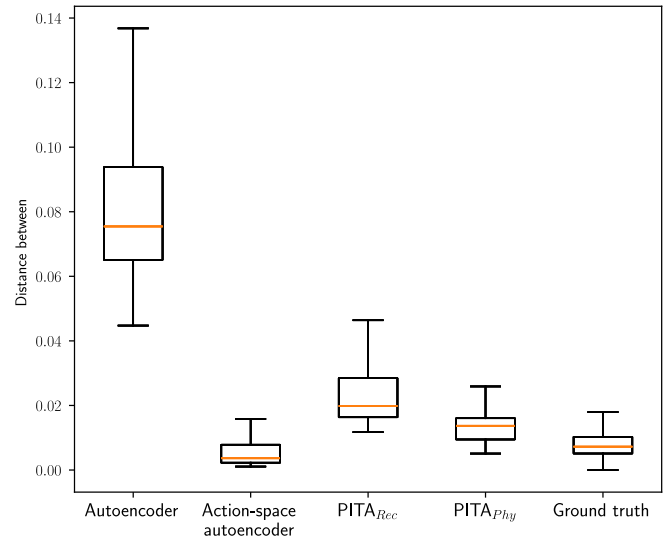


Figure 5: Boxplot of the distance of the predicted positions to the corresponding smoothed reference path.

To the best of our knowledge, this is the first work to incorporate physics-informed machine learning principles into trajectory encoding and prediction. These concepts allow to learn an encoder that captures not only the future positions, but also the dynamic properties on the system. Based on the learned physics-informed encoder, we can train generative models that produce physically plausible and realistic trajectories for data augmentation.

In contrast to common prediction approaches, our framework predicts output trajectory points at a high temporal resolution of 25 Hz. On the one hand this is necessary to augment data with high-fidelity. On the other hand, this is prone to result in nonsmooth predictions due to the inherent prediction uncertainty.

Based on this work, our future research will focus on incorporating additional context information on the traffic scene into the model. This allows to encode the whole traffic scene instead of only a single vehicle’s trajectory.

REFERENCES

- [1] A. Ramesh, M. Pavlov, G. Goh, S. Gray, C. Voss, A. Radford, M. Chen, and I. Sutskever, “Zero-Shot Text-to-Image Generation,” in *Proceedings of the 38th International Conference on Machine Learning*. PMLR, Jul. 2021, pp. 8821–8831.
- [2] R. Rombach, A. Blattmann, D. Lorenz, P. Esser, and B. Ommer, “High-Resolution Image Synthesis With Latent Diffusion Models,” in *Proceedings of the IEEE/CVF Conference on Computer Vision and Pattern Recognition*, 2022, pp. 10 684–10 695.
- [3] F. Janjos, M. Dolgov, and J. M. Zollner, “Self-Supervised Action-Space Prediction for Automated Driving,” in *2021 IEEE Intelligent Vehicles Symposium (IV)*. Nagoya, Japan: IEEE, Jul. 2021, pp. 200–207.
- [4] F. Janjos, M. Dolgov, M. Kuric, Y. Shen, and J. M. Zollner, “SAN: Scene Anchor Networks for Joint Action-Space Prediction,” in *2022 IEEE Intelligent Vehicles Symposium (IV)*. Aachen, Germany: IEEE, Jun. 2022, pp. 1751–1756.
- [5] M. Raissi, P. Perdikaris, and G. Karniadakis, “Physics-informed neural networks: A deep learning framework for solving forward and inverse problems involving nonlinear partial differential equations,” *Journal of Computational Physics*, vol. 378, pp. 686–707, Feb. 2019.

- [6] Z. Mo, X. Di, and R. Shi, "A Physics-Informed Deep Learning Paradigm for Car-Following Models," *Transportation Research Part C: Emerging Technologies*, vol. 130, p. 103240, Sep. 2021.
- [7] H. Naing, W. Cai, J. Yu, T. Wu, and L. Yu, "Physics-guided graph convolutional network for modeling car-following behaviors under distributional shift," Sep. 2023, pp. 2574–2581.
- [8] J. Fischer, A. Trofimov, and C. Stiller, "Physics-informed Reinforcement Learning for Automated Merging in Dense Traffic," in *15. Workshop Fahrerassistenz Und Automatisiertes Fahren (FAS)*. Berkheim, Germany: Uni-DAS e.V., Oct. 2023, pp. 43–51.
- [9] P. Maheshwari, W. Wang, S. Triest, M. Sivaprakasam, S. Aich, J. G. Rogers III, J. M. Gregory, and S. Scherer, "PIAug – Physics Informed Augmentation for Learning Vehicle Dynamics for Off-Road Navigation," Nov. 2023.
- [10] R. Krajewski, J. Bock, L. Kloeker, and L. Eckstein, "The highD Dataset: A Drone Dataset of Naturalistic Vehicle Trajectories on German Highways for Validation of Highly Automated Driving Systems," in *2018 21st International Conference on Intelligent Transportation Systems (ITSC)*. Maui, HI: IEEE, Nov. 2018, pp. 2118–2125.
- [11] R. Krajewski, T. Moers, J. Bock, L. Vater, and L. Eckstein, "The roundD Dataset: A Drone Dataset of Road User Trajectories at Roundabouts in Germany," in *2020 IEEE 23rd International Conference on Intelligent Transportation Systems (ITSC)*. Rhodes, Greece: IEEE, Sep. 2020, pp. 1–6.
- [12] W. Zhan, L. Sun, D. Wang, H. Shi, A. Clausse, M. Naumann, J. Kümmerle, H. Königshof, C. Stiller, A. de La Fortelle, and M. Tomizuka, "INTERACTION Dataset: An INTERnational, Adversarial and Cooperative moTION Dataset in Interactive Driving Scenarios with Semantic Maps," *arXiv:1910.03088 [cs, eess]*, 2019.
- [13] H. M. T. Menegaz, J. Y. Ishihara, G. A. Borges, and A. N. Vargas, "A Systematization of the Unscented Kalman Filter Theory," *IEEE Transactions on Automatic Control*, vol. 60, no. 10, pp. 2583–2598, Oct. 2015.